Brazilian Journal of Physics
ISSN: 0103-9733
luizno.bjp@gmail.com
Sociedade Brasileira de Física
Brasil

Pugliesi, R.; Pugliesi, Fábio; Stanojev Pereira, M. A.
Comparison of Digital Imaging Systems for Neutron Radiography
Brazilian Journal of Physics, vol. 41, núm. 2-3, septiembre, 2011, pp. 123-128
Sociedade Brasileira de Física
São Paulo, Brasil

Available in: http://www.redalyc.org/articulo.oa?id=46421602005

- How to cite
- Complete issue
- More information about this article
- Journal's homepage in redalyc.org

Scientific Information System
Network of Scientific Journals from Latin America, the Caribbean, Spain and Portugal
Non-profit academic project, developed under the open access initiative

Braz J Phys (2011) 41:123–128
DOI 10.1007/s13538-011-0016-3

SBF SOCIEDADE BRASILEIRA DE FÍSICA

GENERAL AND APPLIED PHYSICS

Comparison of Digital Imaging Systems for Neutron Radiography

R. Pugliesi · Fábio Pugliesi · M. A. Stanojev Pereira

Received: 31 January 2011 / Published online: 14 April 2011
© Sociedade Brasileira de Física 2011

Abstract The characteristics of three digital imaging systems for neutron radiography purposes have been compared. Two of them make use of films, CR-39 and Kodak AA, and the third makes use of a LiF scintillator, for image registration. The irradiations were performed in the neutron radiography facility installed at the IEA-R1 nuclear research reactor of IPEN-CNEN/SP. According to the obtained results, the system based on CR-39 is the slowest to obtain an image, and the best in terms of resolution but the worse in terms of contrast. The system based on Kodak AA is faster than the prior, exhibits good resolution and contrast. The system based on the scintillator is the fastest to obtain an image, and best in terms of contrast but the worse in terms of resolution.

Keywords Imaging systems · Neutron radiography · Digital image

1 Introduction

The neutron radiography (NR) is a well-known non-destructive testing technique. The radiography is obtained by irradiating a sample with a uniform neutron beam. A converter screen transforms the transmitted neutron intensity into a radiation able to sensitize a film or a scintillator, forming the image of the sample [1–3]. Usually, the images are digitized by using a video camera or a scanner, associated to a software to quantify light transmitted intensity through the sensitized region. These sets are known as digital imaging systems. In the present paper, three different imaging systems, commonly used for neutron radiography, have been studied and some of their characteristics compared with each other. Two are film-based systems and the images are digitized by using a scanner and the third one is a scintillator-based system and the images are digitized by using a video camera. The parameters used to compare them were the mean contrast value, neutron exposure to obtain the best contrast, capability to discern thickness of the materials, and spatial resolution. The light transmitted intensity was evaluated in an 8 bits gray-level (GL) scale ranging from 0 to the darkest pixel to 255 to the brightest one [4–6].

2 Experimental

The irradiations were performed at the neutron radiography facility installed at the beam-hole #8 of the pool-type IEA-R1 nuclear research reactor of IPEN-CNEN/SP. The characteristics of the neutron beam at the irradiation position are shown in Table 1.

The first imaging system consists of a natural boron converter screen associated to a film, the solid-state nuclear track detector CR-39. During irradiation, the screen and the film are kept in a tight contact inside an aluminum cassette and the neutron–boron interaction generates 1.47 MeV alpha particles which will sensitize the film. After film development, the light

R. Pugliesi (✉) · Fábio Pugliesi
Centro do Reator de Pesquisas-CRPq–Divisão de Física Nuclear, Instituto de Pesquisas Energéticas e Nucleares (IPEN-CNEN/SP), 05508 170, Sao Paulo, Brazil
e-mail: pugliesi@ipen.br

M. A. Stanojev Pereira
Instituto Tecnológico e Nuclear, Estrada Nacional 10, 2686-953 Sacavém, Portugal

Table 1 Characteristics of the neutron beam at the irradiation position

Flux (n.s^{-1} cm^{-2})	1.75×10^{6}[a]
Beam diameter (cm)	20
Neutron/gamma ratio (n.cm^{-2} mRem^{-1})	8×10^{5}
Mean energy (meV)	7
Homogeneity (%)	10–20

[a]Reactor power at 3.5 MW [5]

transmission readings are performed by using a light transmission scanner and a software [5]. The second consists of a gadolinium converter screen associated to a conventional X-ray emulsion film, Kodak AA double coated. During irradiation, the screen and the film are kept in a tight contact inside an evacuated aluminum cassette and the neutron–gadolinium interaction generates 70 KeV conversion electrons which will sensitize the film. After a standard film development procedure, the light transmission readings were performed by using the same scanner and software mentioned above [4, 5]. The third imaging system consists of a ZnS–LiF scintillator converter screen associated to a cooled charge-coupled device (CCD) digital video camera. The neutron–lithium interaction generates 2.05 MeV alpha and 2.74 MeV tritium particles which will sensitize the ZnS, giving rise to scintillations which are captured by the camera [7]. During irradiation the screen and the camera are kept inside an aluminum light tight box. In order to minimize damages in the camera's CCD caused by neutrons and gamma rays, the light generated by the scintillator is reflected by a mirror positioned at 45° with respect to the radiation beam.

3 Data Acquisition and Analysis

3.1 Mean Contrast Value and Exposure to Obtain the Best Contrast in the Image

The contrast is defined by Eq. 1. It is determined by means of curves that relate "gray level (GL)" as functions of the "neutron exposure (E)", given by E (n.cm^{-2}) = ϕ(n.s^{-1} cm^{-2})*t(s) where ϕ is the neutron flux at the irradiation position and t is the irradiation time.

$$G = \mathrm{d(GL)/d(logE)} \tag{1}$$

The mean contrast value corresponds to the slope of the straight line fitted to the steeper region of the "GL *vs* E" curves and the exposure to obtain the best contrast in the image is the one corresponding to the end of the steeper region. The curves for the studied

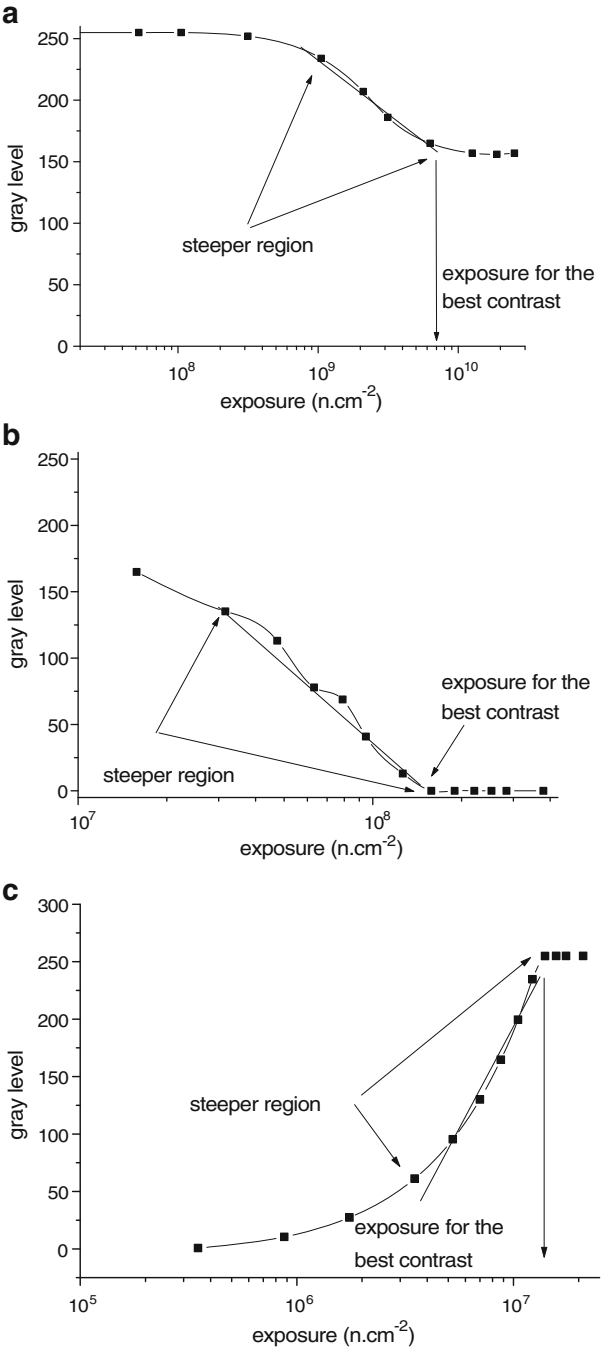

Fig. 1 Gray level as functions of the neutron exposure for the **a** CR-39, **b** Kodak AA, and **c** scintillator imaging systems

Table 2 Values for the exposure and contrast for the three studied imaging systems

Imaging system	Exposure (n.cm^{-2})	Mean contrast
CR-39	7.7×10^{9}	90 ± 6
Kodak AA	1.5×10^{8}	226 ± 15
Scintillator	1.4×10^{7}	330 ± 26

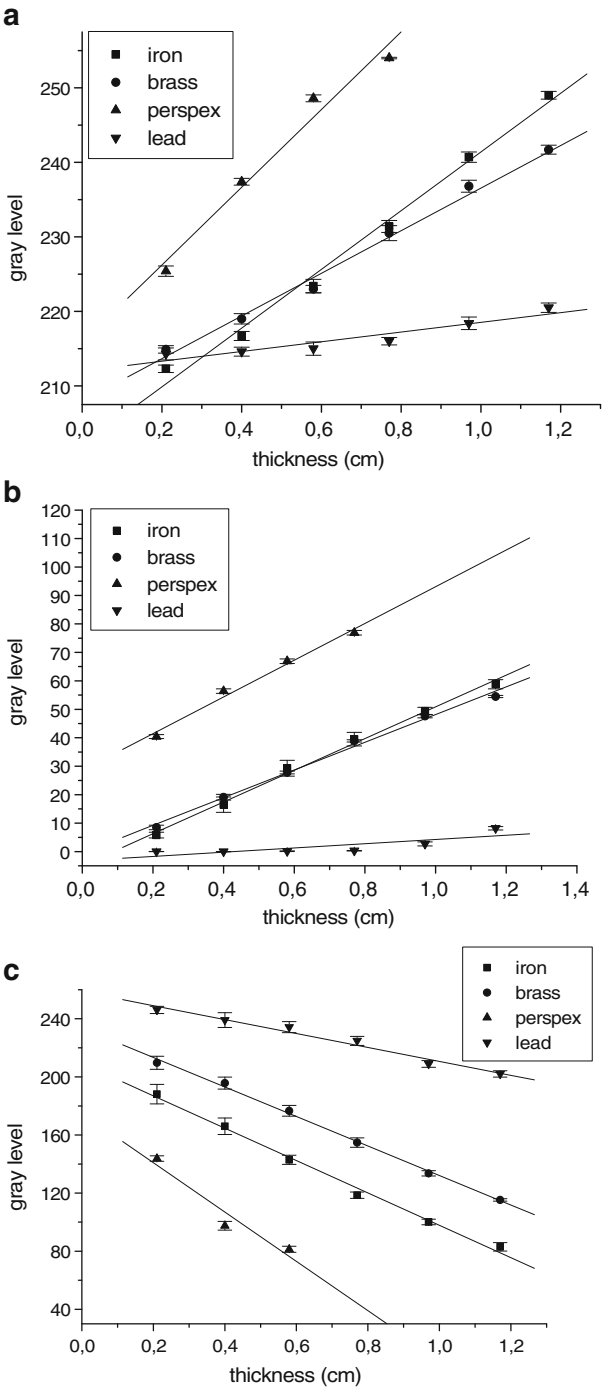

Fig. 2 Gray level as functions of the sample thickness for the **a** CR-39, **b** Kodak AA, and **c** scintillator imaging systems

imaging systems, shown in the Fig. 1a–c, have been obtained by irradiating the converter screens in the direct neutron beam (without sample).

The evaluated parameters are indicated in the figures and given in Table 2.

According to the results, the CR-39 system provides the worst images in terms of contrast and requires the greatest exposure. Based in the exposure value, the irradiation time to obtain an image is 67 min. By taking into account the time spent for film development, washing, drying, and scanning, the overall time spent to obtain an image is about 110 min. The Kodak AA system provides better contrast images than the CR-39, the irradiation time is 1.5 min and the overall time is about 70 min. The scintillator system provides the best images in terms of contrast and since development is not necessary, the images are captured simultaneously to their formation and the overall time is about 0.13 min.

3.2 Capability to Discern Thickness of Materials

The capability to discern thickness was evaluated in terms of the minimal discernible thickness of a material, as follows [8]. For radiography purposes, the neutron transmission by matter is given by the following exponential law [9]:

$$\phi(x) = \phi_0 \cdot \exp(-\Sigma_{\text{eff}} \cdot x) \tag{2}$$

where ϕ_0 and $\phi(x)$ are the incident and transmitted neutron fluxes through the sample, having thickness "x" and effective total macroscopic cross-section "Σ_{eff}" which takes into account the contribution of the neutrons scattered by the sample to the image formation [10].

For images obtained in the best contrast region, where GL = G log(E), the gray level as a function of the material thickness, is given by the following linear function [1, 4]:

$$\text{GL} = \text{GL}_0 - S \cdot x \tag{3}$$

where $S = 0.43\ \text{G}\ \Sigma_{\text{eff}}$ and GL_0 is the gray level for zero thickness.

The discernible thickness of a material can be evaluated from Eq. 3 as:

$$\Delta x = \Delta\text{GL}/S \tag{4}$$

where ΔGL is the gray level variation in the image.

Table 3 Values for the minimal discernible thickness for the three studied imaging systems

Imaging system	Min ΔGL	Minimal discernible thickness (cm)			
		Iron	Brass	Perspex	Lead
CR-39	7.5	0.19 ± 0.01	0.26 ± 0.01	0.14 ± 0.02	1.2 ± 0.2
Kodak AA	6.7	0.120 ± 0.004	0.14 ± 0.01	0.10 ± 0.01	0.9 ± 0.3
Scintillator	2.7	0.024 ± 0.001	0.027 ± 0.001	0.016 ± 0.004	0.056 ± 0.005

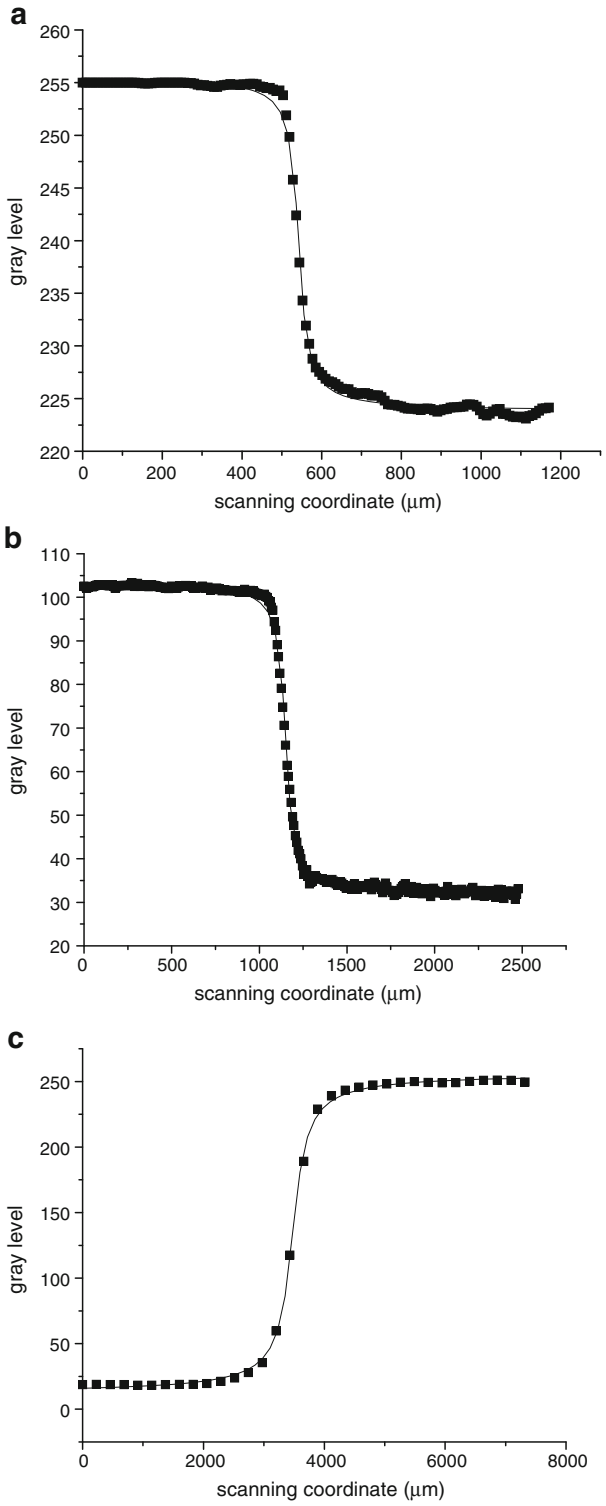

Fig. 3 Gray level as functions of the scanning coordinate for the **a** CR-39, **b** Kodak AA, **c** scintillator imaging systems

The minimal discernible thickness is evaluated by Eq. 4, by taking ΔGL as the minimal discernible gray level variation by the imaging system [8]. It was determined for the materials, iron, brass, Perspex and lead. The samples are step wedges with thicknesses varying between 2 and 12 mm, which have been irradiated as close as possible to the converter screens and at the exposures for which the best contrasts were achieved (see Table 2). Figure 2a–c show the behavior of the gray level as functions of the sample thickness for the three studied imaging systems as well as the fit of Eq. 3 to the data sets. The obtained results for the minimal discernible thickness and for the minimal discernible gray level variation are shown in Table 3.

The scintillator system exhibits the best capability to discern thickness of materials. This is expected because besides presenting the best mean contrast, the value of ΔGL is at least 2.5 times smaller than the value for the two other imaging systems.

3.3 Spatial Resolution

In radiography, the spatial resolution is defined as the minimum distance that two objects must be separated before they can be distinguished from each other [11]. Since the particles emitted by the converters (alphas, protons, and electrons) are randomly distributed in all directions, they will sensitize the film or the scintillator in an area greater than the area from which they originate. Hence, the resolution depends on [12]:

A. Sample thickness
B. Sample to film(scintillator) distance
C. Film(scintillator) grain size
D. Range of the particles in the converter and in the film (scintillator)

The resolution is usually quoted in terms of the total unsharpness (Ut) and is obtained by scanning the light distribution at the interface between the images of a neutron opaque sample and the one corresponding to the direct neutron beam. An edge spread function Eq. 5, is fitted to the resulting distribution and the total unsharpness is given by Eq. 6 [13, 14].

$$\mathrm{GL} = p1 + p2(\arctan(p3\ (X - p4))) \tag{5}$$

Table 4 Values for the resolution for the three studied imaging systems

Imaging system	Ut (micrometers)
CR-39	33 ± 1
Kodak AA	67 ± 1
Scintillator	357 ± 15

where X is the scanning coordinate and p_1, p_2, p_3, and p_4 are free parameters in the fit.

The total unsharpness is given by

$$\mathrm{Ut} = 2/(p3) \tag{6}$$

The opaque sample used was a 100 μm cadmium strip which was irradiated as close as possible to the converter screens and at the exposures for which the best contrasts were determined (see Table 2). The Fig. 3a–c show the obtained distributions for the imaging systems as well as the fit of Eq. 5 to the data.

The obtained results for Ut are shown in Table 4. As can be seen, the CR-39 system presents the best resolution followed by the Kodak AA, and by the scintillator system. These results are in accordance to the mentioned above because since A and B are the same for the three studied imaging systems the resolution depends on C and D and in such case both parameters are smaller for the CR-39 system.

4 Conclusions

Based on the obtained results we can underline the following conclusions:

- The CR-39 system exhibits the worst contrast and the worst capability to discern thickness of the materials. However, this system is able to provide the best image in terms of spatial resolution. It is also worth mentioning that because of the large time spent for irradiation, development procedures, scanning, and film price, the obtainment of an image is the most expensive. However, the overall cost can eventually be reduced by using a polymer manufactured in country, like the Durolon [5].
- The Kodak AA system provides intermediate values for the studied parameters when compared with the CR-39 and scintillator systems. Furthermore, by considering the overall time spent to obtain the image and the film price, the cost to obtain in an image is somewhat smaller than the CR-39 system.
- The scintillator system provides the best contrast and the best capability to discern thickness of the materials, however the worst image in terms of resolution. This system also offers the smallest irradiation time and since it is not necessary neither film development nor scanning to digitize the image it provides the smallest cost. However, if we consider the prices of the LiF scintillator and of a cooled CCD video camera, the initial cost to install this system is relatively high when compared with the other two.

In order to illustrate the characteristics of the studied systems, Fig. 4a–c shows images of same sample (a 5-mm hole in a cadmium strip), obtained by using the CR-39, Kodak AA, and scintillator imaging systems respectively. Figure 4a exhibits the lowest contrast but the highest resolution since the edge of the hole is sharply defined, Fig. 4b exhibits good contrast and good resolution, and Fig. 4c exhibits the best contrast but the lowest resolution since the edges of the hole are not well defined.

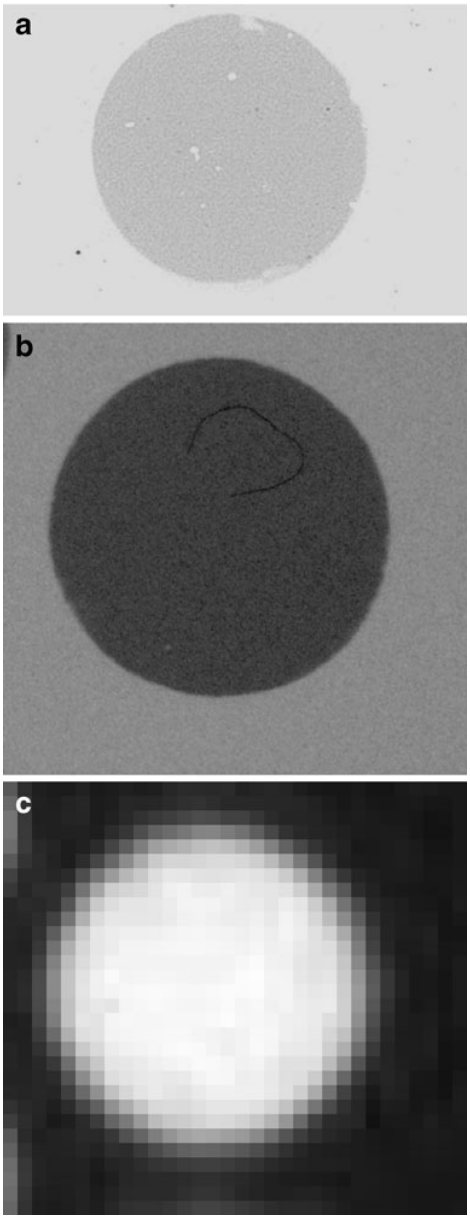

Fig. 4 Images of a hole in a cadmium strip obtained by using the **a** CR-39, **b** Kodak AA, and **c** scintillator imaging systems

Acknowledgements The authors thank the financial support provided by "FAPESP (project 09502610)" to acquire the digital image processing system used to quantify the parameters.

References

1. P. von Der Hardt, H. Roettger, *Neutron Radiography Handbook: Nuclear Science and Technology* (D. Reidl, Dordrecht, 1981)
2. H. Berger, *Neutron Radiography, Methods, Capabilities and Applications* (Elsevier, New York, 1965)
3. G. Bayon, Applications of neutron radiography in France, in *3rd International Topical Meeting on NR. Lucerne, Switzerland, 16-19 March* (1998)
4. R. Pugliesi, M.L.G. Andrade, M.A. Stanojev Pereira, F. Pugliesi, Nucl. Instrum. Methods Phys. Res. **A 542**, 81–86 (2005)
5. F. Pugliesi, Characterization of Durolon as a solid state nuclear detector. PhD Thesis. CNEN/SP (2008)
6. M.A. Stanojev Pereira, R. Pugliesi, F. Pugliesi, Radiat. Meas. **43**(7), 1226–1230 (2008)
7. M.R. Hawkesworth. Atom. Energy Rev. **152,** 169–220 (1977)
8. R. Pugliesi, M.A. Stanojev Pereira. Radiat. Meas. **37**(2), 103–195 (2002)
9. L.F. Curtiss, *Introduction to Neutron Physics* (D. van Nostrand Co. Inc., Princenton, New Jersey, 1959)
10. H. Kobayashi, A correlated study between effective total macroscopic cross section and effective energies for continuos neutron beams. in *3rd International Topical Meeting on NR. Lucerne, Switzerland, 16–19 March* (1998)
11. R. Ilic', M. Najzer, Nucl. Track Radiat. Meas. **17**, 475–481 (1990)
12. R.H. Herz, *The Photographic Action of Ionizing Radiation*. (Wiley, New York, 1968)
13. A.A. Harms, A.A. Zellinger, Phys. Med. Biol. **22**(1), 70–80 (1977)
14. M. Wrobel, L. Greim, Geesthacht, German, GKSS, (GKSS 88/e/12) (1988)